

## Supporting Information

### Boosting the Photodynamic Degradation of Islet Amyloid

### Polypeptide Aggregates via a “Bait-Hook-Devastate” Strategy

*Yujuan Cao<sup>†</sup>, Zhenyan He<sup>†</sup>, Yuting Gao<sup>†</sup>, Yanru Xin<sup>†</sup>, Liang Luo<sup>†,‡</sup>, Fanling Meng<sup>†,‡\*</sup>*

<sup>†</sup>National Engineering Research Center for Nanomedicine, College of Life Science and Technology, Huazhong University of Science and Technology, Wuhan, 430074, China

<sup>‡</sup>Hubei Key Laboratory of Bioinorganic Chemistry and Materia Medica, School of Chemistry and Chemical Engineering, Huazhong University of Science and Technology, Wuhan 430074, China

\*Corresponding author: [fanlingmeng@hust.edu.cn](mailto:fanlingmeng@hust.edu.cn)

Contents	Pages
1. Figure S1	S-2
2. Figure S2	S-3
3. Figure S3	S-4
4. Figure S4	S-5
5. Figure S5	S-6
6. Figure S6	S-7
7. Figure S7	S-8
8. Figure S8	S-9
9. Figure S9	S-10
10. Figure S10	S-11

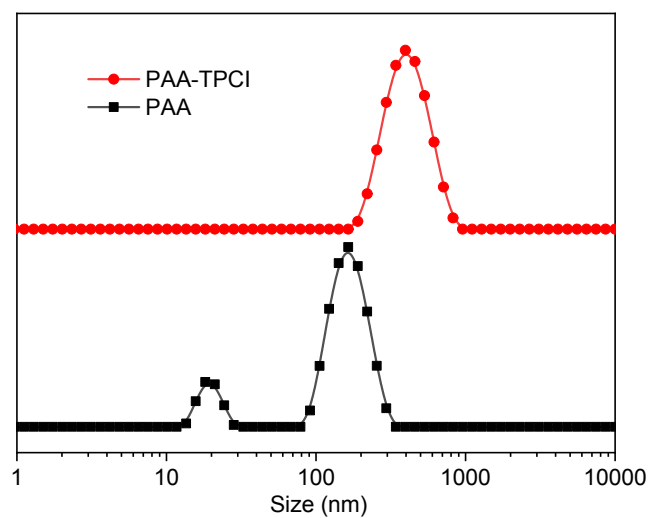


**Figure S1.** Particle size distributions of PAA and PAA-TPCI measured by DLS. The concentrations of PAA and TPCI were  $1.28 \mu\text{M}$  and  $8 \mu\text{M}$  respectively.

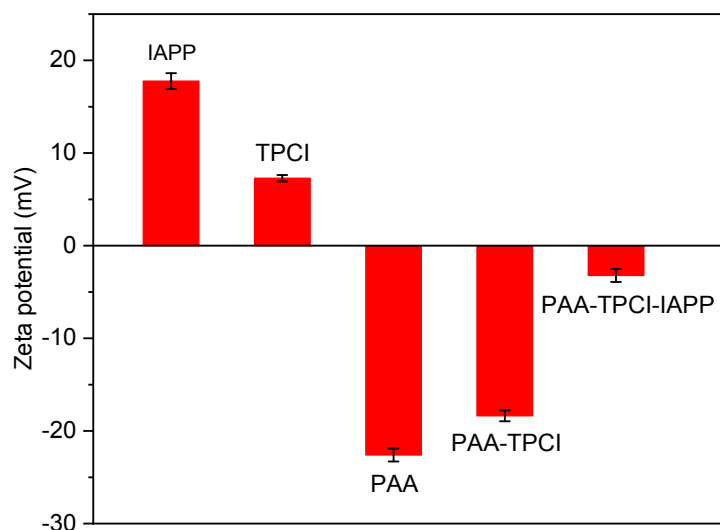


**Figure S2.** Zeta potential of IAPP aggregates (IAPP), TPCI, PAA, and complexes. The concentrations of IAPP aggregates, PAA, TPCI were 32  $\mu\text{M}$ , 1.28  $\mu\text{M}$  and 8  $\mu\text{M}$ , respectively when measured separately. The concentrations of PAA and TPCI in PAA-TPCI were 0.018  $\mu\text{M}$  and 0.11  $\mu\text{M}$  respectively. The concentrations of PAA, TPCI and IAPP aggregates in PAA-TPCI-IAPP were 0.018  $\mu\text{M}$ , 0.11  $\mu\text{M}$ , 32  $\mu\text{M}$  respectively.

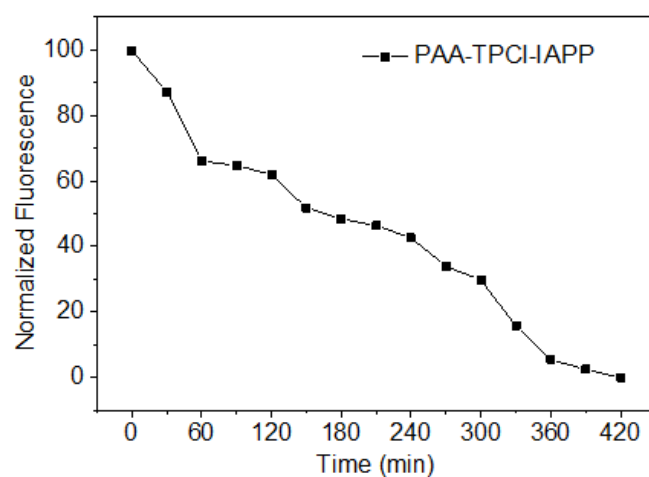


**Figure S3.** ThT fluorescence kinetics of IAPP aggregates in the presence of PAA and TPCI (PAA-TPCI-IAPP) upon LED light illumination in water instead of tris-HCl buffer. The concentrations of IAPP aggregates and TPCI were 32  $\mu$ M and 8  $\mu$ M respectively.

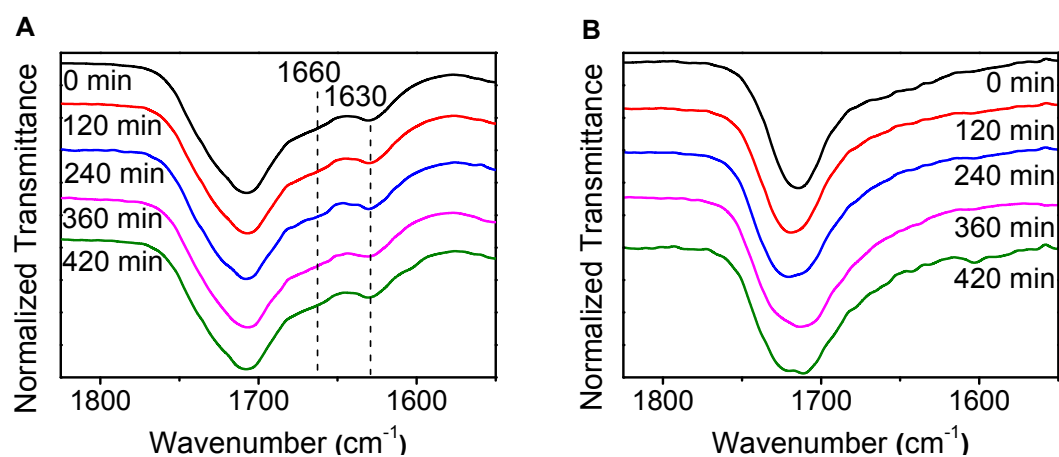


**Figure S4.** FTIR spectra of PAA-IAPP (A), PAA-TPCI (B) under different illumination time points. The concentrations of IAPP aggregates and TPCI were 32  $\mu\text{M}$  and 8  $\mu\text{M}$  respectively.

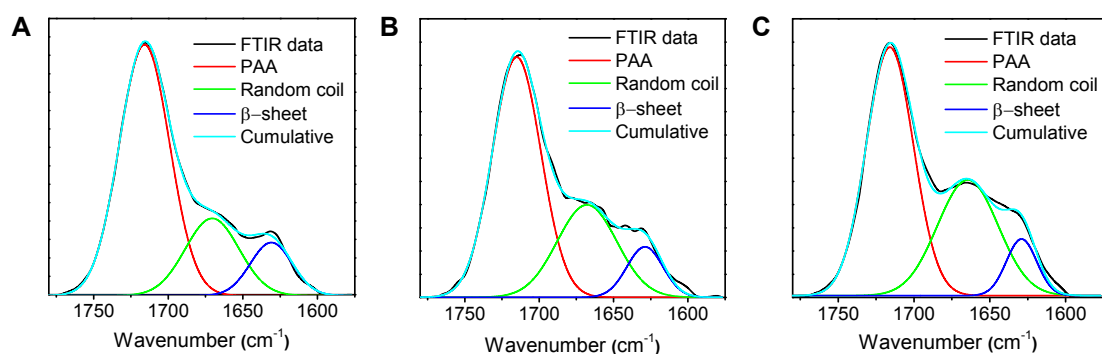


**Figure S5.** FTIR multiple-peak fit spectra of the PAA-TPCI-IAPP sample after being irradiated for 120 min (A), 240 min (B) and 360 min (C). The concentrations of IAPP aggregates and TPCI were 32  $\mu$ M and 8  $\mu$ M respectively.

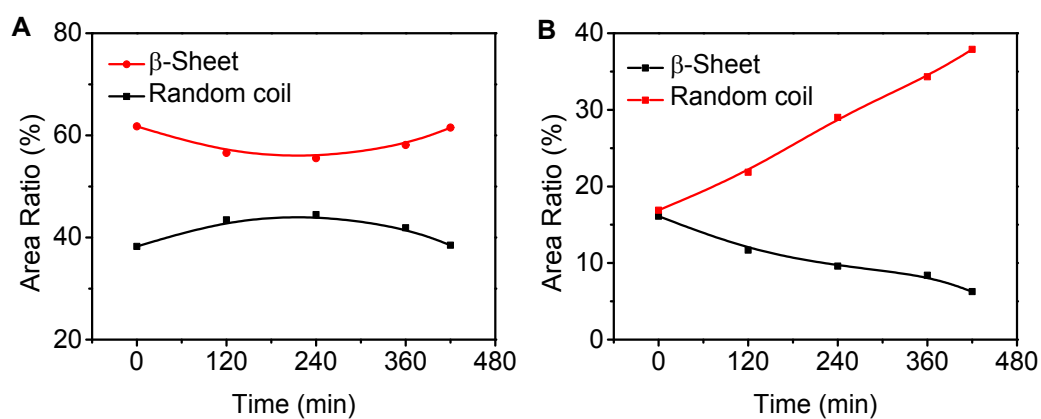


**Figure S6.** The changes of random coil and  $\beta$ -sheet peak area ratio of TPCI-IAPP (A) and PAA-TPCI-IAPP (B) samples in FTIR multi-peak fitting spectrum at different illumination time points. The concentrations of IAPP aggregates and TPCI were  $32\ \mu\text{M}$  and  $8\ \mu\text{M}$  respectively.

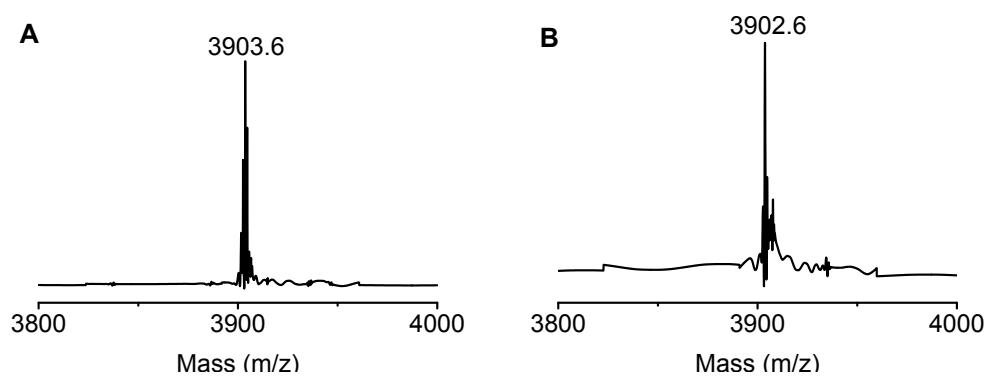


**Figure S7.** MALDI-TOF MS spectra of the PAA-IAPP sample before irradiation (A) and after 90 min of irradiation (B). The concentrations of IAPP aggregates and PAA were 8  $\mu\text{M}$  and 0.32  $\mu\text{M}$  respectively.



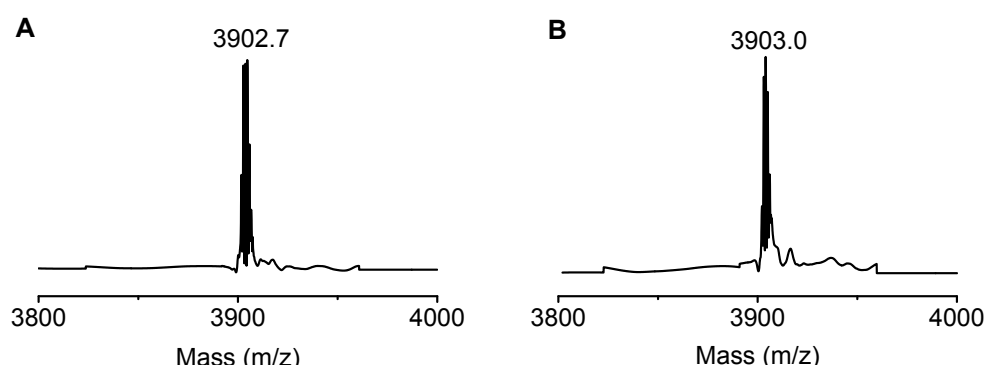


**Figure S8.** MALDI-TOF MS spectra of the TPCI-IAPP sample before irradiation (A) and after 90 min of irradiation (B). The concentrations of IAPP aggregates and TPCI were 8  $\mu$ M and 2  $\mu$ M respectively.

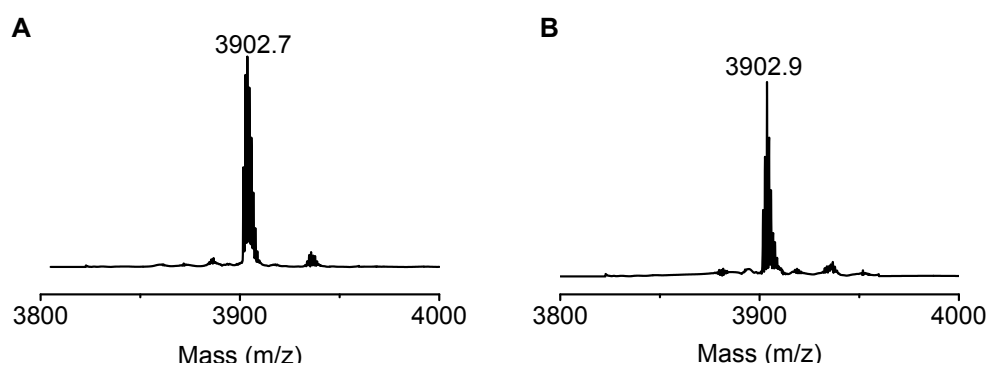


**Figure S9.** MALDI-TOF MS spectra of the IAPP sample before irradiation (A) and after 90 min of irradiation (B). The concentration of IAPP aggregates was 8  $\mu$ M.

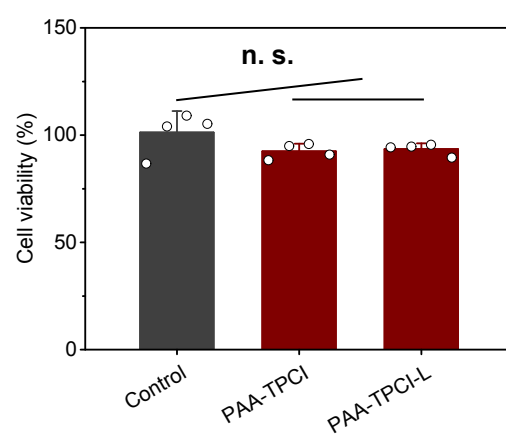


**Figure S10.** Cell viability of PAA-TPCI without and with light irradiation (16 mW cm<sup>-2</sup>, 90 min).